AD-A134 327 WHISTLER MODE INTERACTIONS AND PLASMA SHEET ELECTRONS 1/1
(U) AEROSPACE CORP EL SEGUNDO CA B C EDGAR ET AL.
18 SEP 83 TR-0083(3940-06)-2 SD-TR-83-62

UNCLASSIFIED F04701-82-C-0083 F/G 20/14 NL

END
DATE
FILMED
-83
DTIC

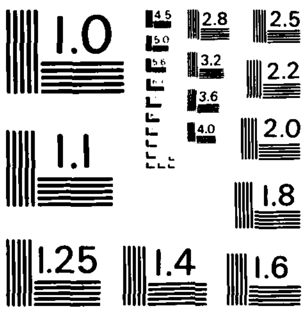

MICROCOPY RESOLUTION TEST CHART
NATIONAL BUREAU OF STANDARDS - 1963 - A

AD-A135 327

(12)

REPORT SD-TR-83-62

Whistler Mode Interactions and Plasma Sheet Electrons

B. C. EDGAR and H. C. KOONS
Space Sciences Laboratory
Laboratory Operations
The Aerospace Corporation
El Segundo, Calif. 90245

18 September 1983

APPROVED FOR PUBLIC RELEASE;
DISTRIBUTION UNLIMITED

Prepared for

SPACE DIVISION
AIR FORCE SYSTEMS COMMAND
Los Angeles Air Force Station
P.O. Box 92960, Worldway Postal Center
Los Angeles, Calif. 90009

This report was submitted by The Aerospace Corporation, El Segundo, CA 90245, under Contract No. F04701-82-C-0083 with the Space Division, P.O. Box 92960, Worldway Postal Center, Los Angeles, CA 90009. It was reviewed and approved for The Aerospace Corporation by H. R. Rugge, Director, Space Sciences Laboratory. Captain Gary Rowe, SD/YC, was the project officer for Mission Oriented Investigation and Experimentation Programs.

This report has been reviewed by the Public Affairs Office (PAS) and is releasable to the National Technical Information Service (NTIS). At NTIS, it will be available to the general public, including foreign nationals.

This technical report has been reviewed and is approved for publication. Publication of this report does not constitute Air Force approval of the report's findings or conclusions. It is published only for the exchange and stimulation of ideas.

Gary M. Rowe

Gary Rowe, Captain, USAF
Project Officer

Joseph Hess

Joseph Hess, GM-15, Director
West Coast Office, AF Space Technology Center

UNCLASSIFIED

SECURITY CLASSIFICATION OF THIS PAGE (When Data Entered)

REPORT DOCUMENTATION PAGE

READ INSTRUCTIONS BEFORE COMPLETING FORM

1. REPORT NUMBER
SD-TR-83-62

2. GOVT ACCESSION NO.
AD-A134327

3. RECIPIENT'S CATALOG NUMBER

4. TITLE (and Subtitle)
WHISTLER MODE INTERACTIONS WITH PLASMA SHEET ELECTRONS

5. TYPE OF REPORT & PERIOD COVERED

6. PERFORMING ORG. REPORT NUMBER
TR-0083(3940-06)-2

7. AUTHOR(s)
Bruce C. Edgar and Harry C. Koons

8. CONTRACT OR GRANT NUMBER(s)
F04701-82-C-0083

9. PERFORMING ORGANIZATION NAME AND ADDRESS
The Aerospace Corporation
El Segundo, Calif. 90245

10. PROGRAM ELEMENT, PROJECT, TASK AREA & WORK UNIT NUMBERS

11. CONTROLLING OFFICE NAME AND ADDRESS
Space Division
Air Force Systems Command
Los Angeles, Calif. 90009

12. REPORT DATE
18 September 1983

13. NUMBER OF PAGES
17

14. MONITORING AGENCY NAME & ADDRESS(if different from Controlling Office)

15. SECURITY CLASS. (of this report)
Unclassified

15a. DECLASSIFICATION DOWNGRADING SCHEDULE

16. DISTRIBUTION STATEMENT (of this Report)
Approved for public release; distribution unlimited.

17. DISTRIBUTION STATEMENT (of the abstract entered in Block 20, if different from Report)

18. SUPPLEMENTARY NOTES

19. KEY WORDS (Continue on reverse side if necessary and identify by block number)
Magnetosphere
Plasma sheet
VLF transmitters
Whistler mode

20. ABSTRACT (Continue on reverse side if necessary and identify by block number)

We present a unique set of wave and particle measurements, taken by the S3-3 satellite on 2 August 1976, from which ~~we infer~~ that signals from a ground-based VLF transmitter were ducted up to the equatorial plasma sheet region by a detached region at $L \sim 4.5$. The waves resonated with the 1-keV plasma sheet electrons, producing narrowband emissions that were received in the conjugate hemisphere by the S3-3 satellite at about $L \sim 3$.

DD FORM 1473 (FACSIMILE)

UNCLASSIFIED

SECURITY CLASSIFICATION OF THIS PAGE (When Data Entered)

PREFACE

We would like to thank J. F. Fennell of The Aerospace Corporation for providing the S3-3 particle data and F. S. Mozer of the University of California, Berkeley, for providing the S3-3 electron density data.

The Berkeley group's research was supported by the Office of Naval Research under contract N00014-75-C-0294. This work was supported in part by the Atmospheric Research Section, National Science Foundation, under grant ATM-75-18118, and in part by the U.S. Air Force under contract F04701-82-C-0083.

A-1

CONTENTS

FIGURES

TABLE

Introduction

On August 2, 1976 the vlf receiver aboard the S3-3 satellite in a region between L ~ 2.9 and L ~ 3.4 detected the complex set of vlf emissions shown by Figure 1. The emissions included wideband vlf hiss, chorus, and discrete vlf line radiation. The emission bands were located about the frequencies being transmitted by the Transportable Very-Low-Frequency (TVLF) transmitter (Koons and Dazey, 1974). The transmission experiments were being conducted in the conjugate hemisphere from the satellite, 25 degrees to the east of the magnetic meridian of the satellite. The occurrence of narrow-band emissions and chorus in the S3-3 data during that time period near solar minimum was quite unusual. It differed entirely from other S3-3 observations of vlf transmitter signals reported by Edgar (1980). The unusual nature of the overall observations prompted a closer examination of the energetic particle and plasma density data taken on the same S3-3 pass by other instruments onboard the satellite. The complete analyses, including ray tracing and resonance calculations, show that plasma sheet electrons penetrating to L ~ 4.35 on the nightside interacted with signals from the TVLF transmitter in a whistler duct formed by a detached region of the plasmasphere. Ray paths similar to duct leakage are shown to be responsible for the S3-3 vlf observations at L ~ 3.

Particle Observations

The S3-3 satellite carried an electron electrostatic analyzer (ESA) which measured electron fluxes in the energy range from 0.17 to 8.4 keV as described by Mizera and Fennell (1977). The particle spectrum was sampled once per second, and a pitch angle distribution was obtained in 20 seconds (1 spin period). In Figure 2 count rate data from three energy channels are shown for the satellite pass on August 2, 1976, during which the vlf emissions described in the introduction were observed. The sensitivity of the electron ESA's measurements is limited by the high-energy penetrating particle background. The 2.7 keV channel in Figure 2 exhibits a typical background from the inner and outer radiation zones. For most S3-3 passes through the plasmasphere, the electron ESA channels exhibit a background similar to the 2.7 keV channel in Figure 2. However, on some occasions the low-energy electron flux does exceed the background and exhibits significant enhancements, as shown by the 0.17 and

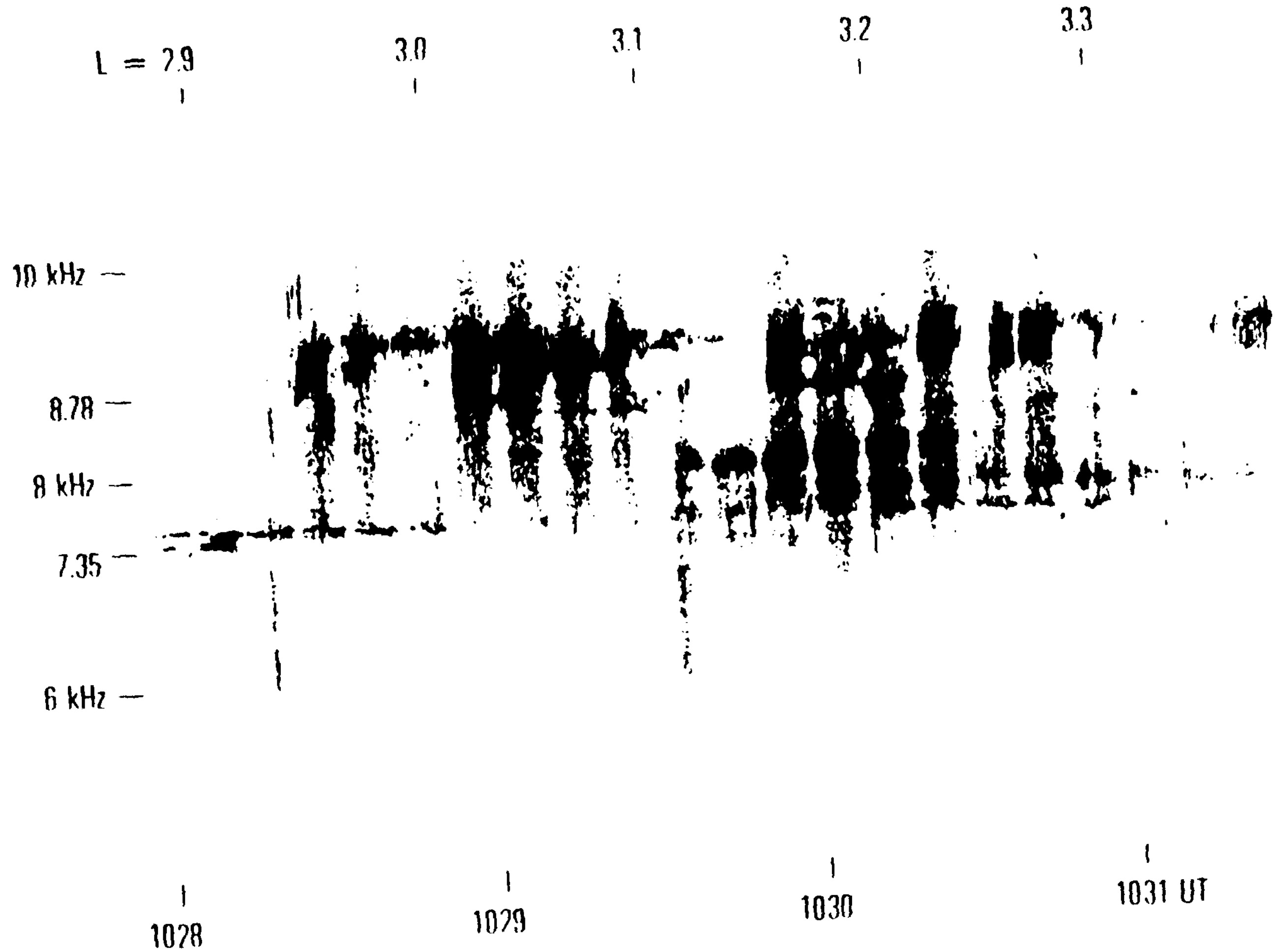

Figure 1. Expanded spectrogram from 6 to 10 kHz of the emissions observed on 2 August 1976 by S3-3. The 8.78 and 7.35 kHz lines identify the TVLF transmitter frequencies during this time.

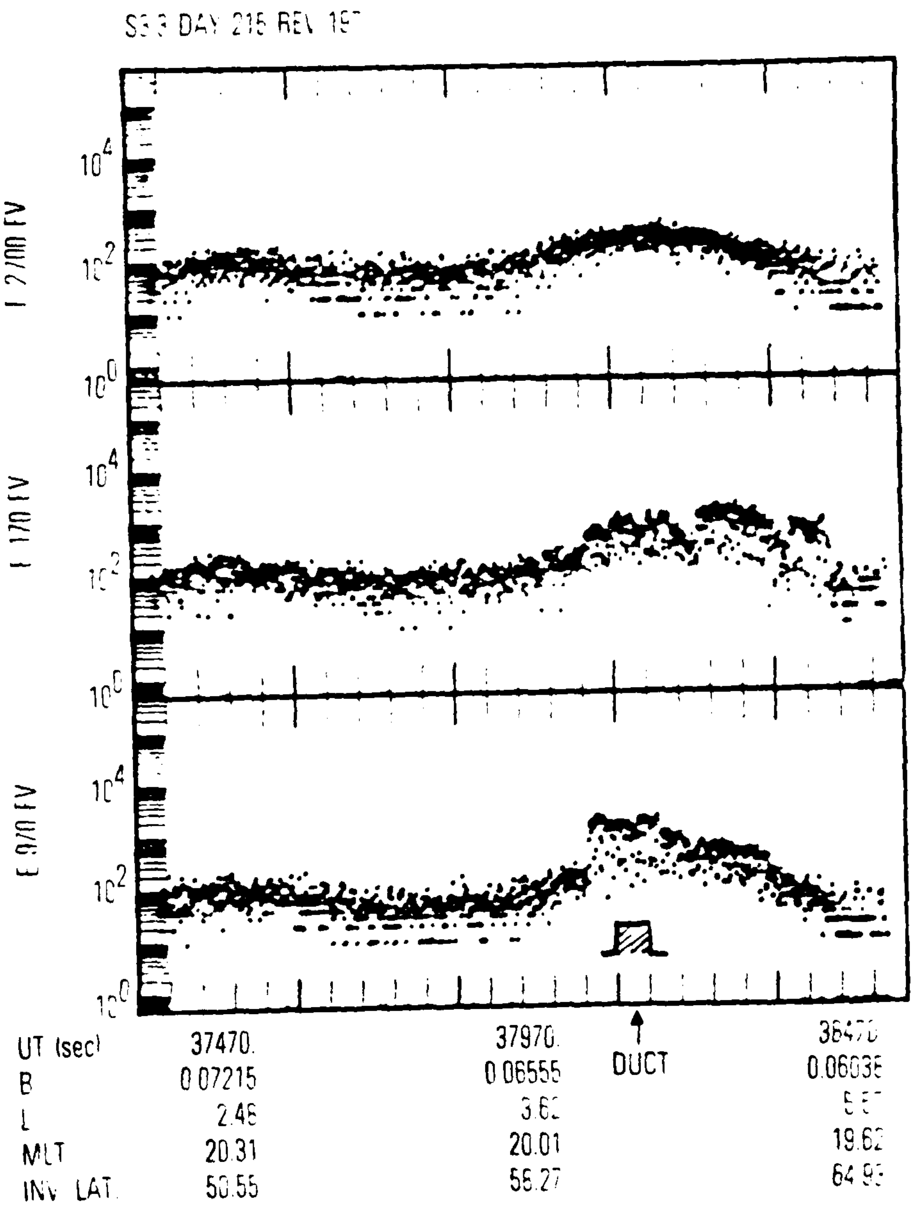

Figure 2. **Time-history of particle counts for 2.7, 0.17, and 0.97 keV electron ESA channels during a S3-3 pass through the plasmasphere on 2 August 1977.**

0.97 keV channels in Figure 2. The low-energy electron flux was measured from L ~ 4.35 to L ~ 6.2. The onset of the 0.97 keV channel at L ~ 4.35 is especially dramatic.

The flux-energy distribution and pitch angle distribution are shown in Figures 3 and 4, respectively, for L ~ 4.5. The angular distribution in Figure 3 shows a typical trapped particle population from 0.17 to 1.6 keV. At the 2.7 keV and higher energy channels, the background causes the data to look isotropic in nature. Therefore the enhancement appears to range between 0.17 and 1.7 keV. Notice the absence of any sign of particle precipitation in Figure 3. In Figure 4 the parallel flux is well below, by an order of magnitude, the trapped flux mirroring at the satellite altitude (6600 km). These low-energy particles are typical of plasma sheet electrons which are injected during a magnetic storm(Fennell et al., 1979).

Density Measurements

The S3-3 satellite also carried a Langmuir probe experiment which used one of the spheres at the ends of the electric field wire boom antennas as the probe (Mozer et al., 1979) A smoothed density profile for electrons is shown in Figure 5. From L ~ 2.6 to 3.8, the density shows a gradual decrease of about an order of magnitude. At L ~ 4.5, there is an enhancement of density which could be interpreted as a detached region of the plasmasphere. This density enhancement is in the region of the enhancement of the low-energy electrons as shown in Figure 2. This juxtaposition suggests that the density enhancement might act as a whistler duct to bring the TVLF transmitter signals to the equator to interact with the low-energy electrons.

Raytracing Calculations

Having established that there is an enhancement of density at L ~ 4.6 and a wide range of low-energy, plasma sheet electrons overlapping the 'duct', we now examine the vlf propagation paths. Assuming a diffusive equilibrium magnetospheric density model, we constructed a density model with a gradual rolloff above L ~ 2.6 and a 100% duct enhancement at L ~ 4.50 with a width of 0.1 L. The density model is also shown in Figure 5. Raypath calculations assumed a starting altitude of 500 km. For ray paths starting at 60.3° lati-

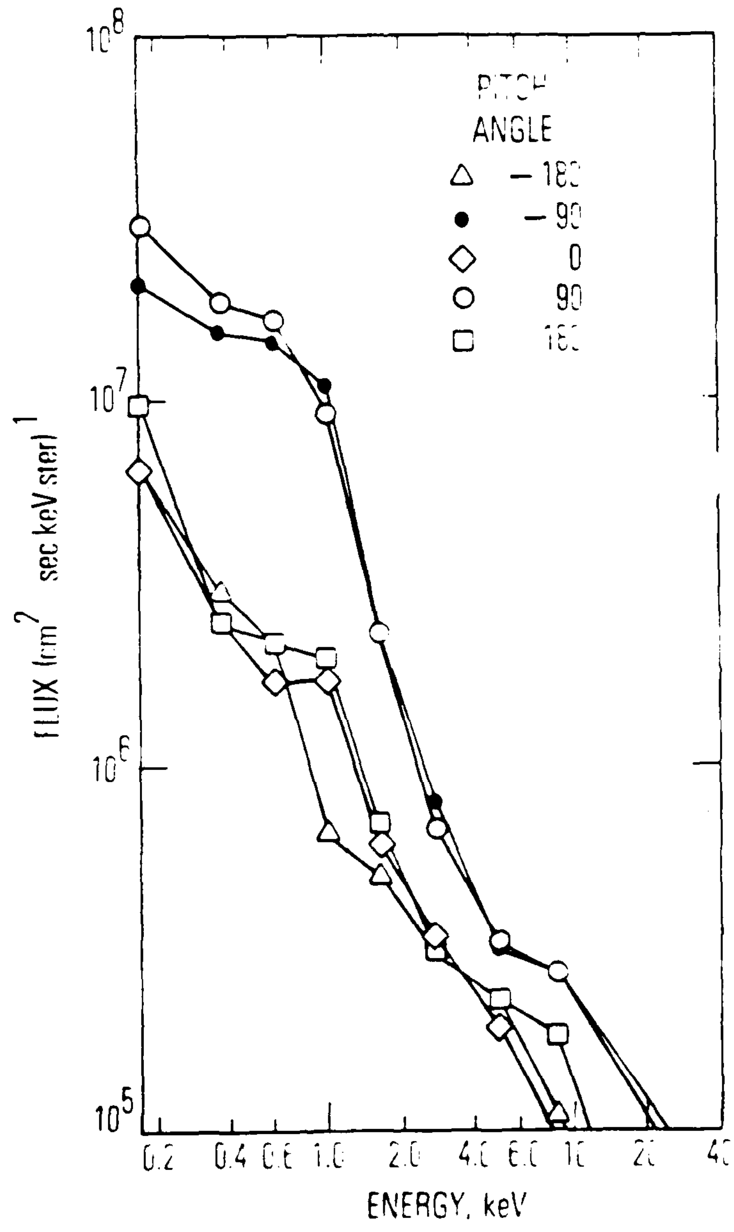

Figure 3. Flux-energy distribution for perpendicular and parallel pitch angles for L ~ 4.5.

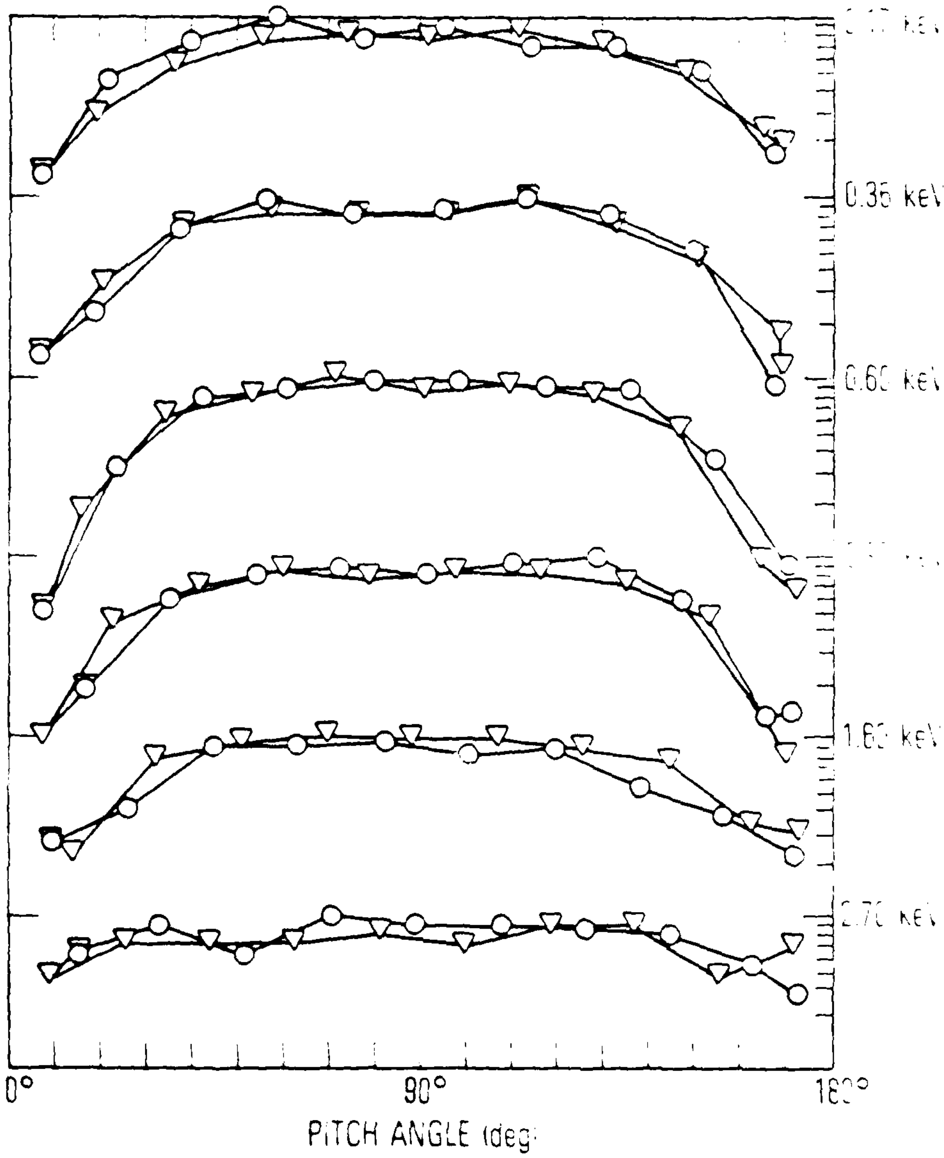

Figure 4. Pitch angle distribution for 0.17 - 2.70 keV electrons observ
at L ~ 4.5 on 2 August 1977.

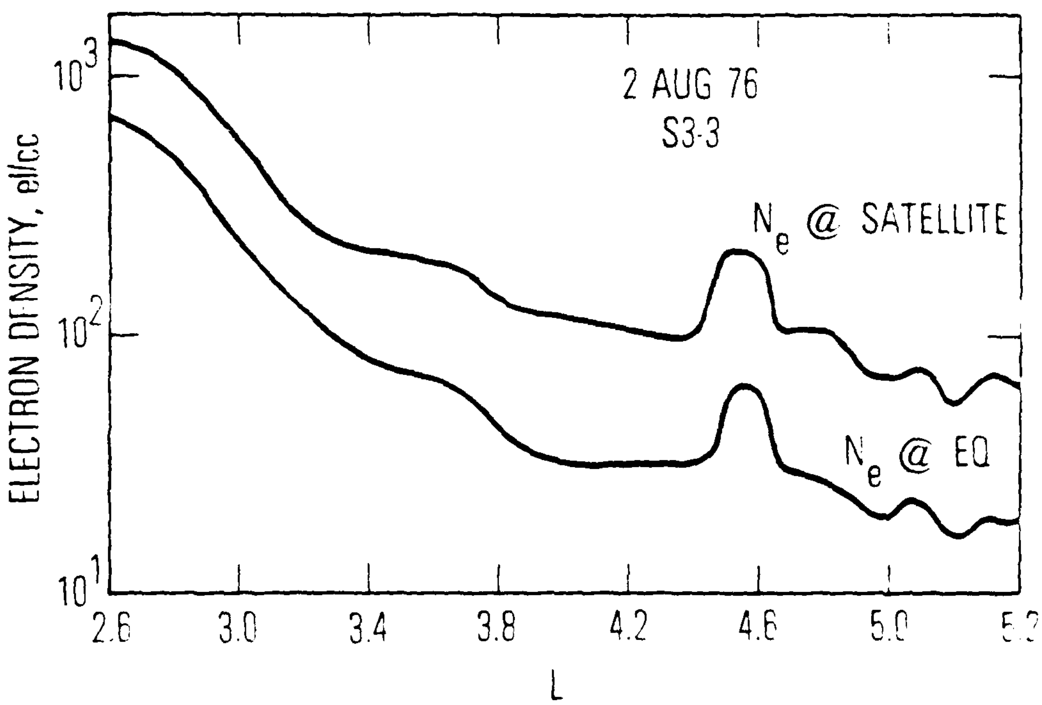

Figure 5. Smoothed electron density profile of the plasmasphere taken by S3-3 on 2 August 1976. The electron density at the equator was scaled from the satellite data using diffusive equilibrium.

tude, the rays are initially trapped by the duct as shown in Figure 6. However at ~ 25,000 km, the signal frequency equals one half the local electron gyrofrequency, and the duct gradients lose control of the wavenormal. The magnetic field curvature gradients then predominate, and the signal "leaks" out of the duct. The wavenormal rotates to a transverse position as the ray traverses the equator. The ray paths eventually intersect the satellite track at L ~ 3. Varying the input latitude slightly causes some minor perturbations in the ray path, but all the rays which are trapped by the duct arrive at the same approximate point along the satellite track as shown in Figure 6.

Using the refractive index values from the raypath calculations in the cyclotron resonance formula

$$\omega - \bar{k} \cdot \bar{v} = \Omega$$

(where ω is the wave frequency, $\bar{k}$ is the wave-number, $\bar{v}$ is the electron velocity, and Ω is the local electron gyrofrequency), we find that the wave can resonate with the plasma sheet electrons along the path as indicated by Figure 6. Indeed, the large variation of the wave normal along the path (as compared to the ducted case) caused by duct leakage allows the wave to resonate with 2 keV to 0.1 keV electrons. Table 1 summarizes the resonance calculations. The waves can resonate with higher energies, but the 0.1 keV lower bound is set by wave conditions at L ~ 4.35 as the ray leaves the particle enhancement. The ray path in Figure 5 was calculated for 8.78 kHz, but the results are essentially the same for 7.35 kHz, the other transmitter frequency.

The duct leakage path to the satellite suggests that the keying pattern (0.5 Hz FSK between 7.35 and 8.78 kHz) might be identified at the point where the signals are first observed. However, no keying pattern was detected.

As mentioned earlier, all the calculated duct-leakage ray paths arrive at nearly the same point along the satellite track. This fact, coupled with no discernable keying pattern and the wide range of observations (L ~ 2.9 to L ~ 3.4) at the satelite, leads to the speculation that the narrow-band emissions and chorus originate near or at the equator, and that transmitter wave-particle interactions control the frequency range and L-shell range of emission activity. Under this assumption, ray tracing calculations were done for

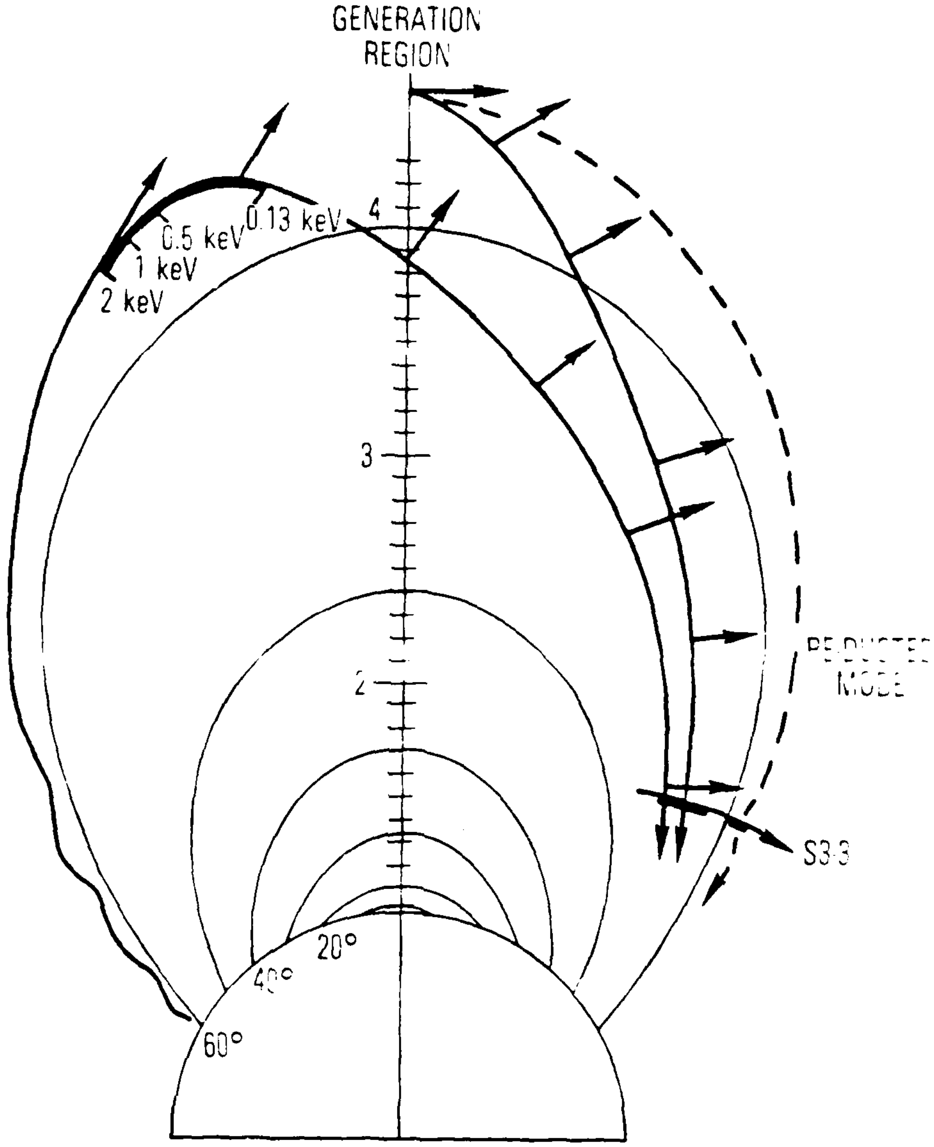

Figure 6. Ray paths for 2 August 1976. A duct exists at $L \sim 4.5$ which initially traps waves entering the magnetosphere at $\theta = 60^{\circ}$. This ray path eventually leaks out of the duct above 25000 km and resonates with 0.1 - 2.0 keV plasma sheet electrons and crosses the satellite track at $L \sim 3$. Using $L_{EQ} \sim 4.5$ as a possible generation region, the other rays show a non-ducted and a reducted mode which could also reach the satellite.

Table 1. Cyclotron Resonance Calculations (8.78 kHz)

L	Lat.	f/f_H	μ	Ψ_{WN}	E (eV)
4.35	8.9°	.724	20.6	-35.9°	130
4.54	15.0°	.680	11.4	- 9.3°	450
4.55	17.4°	.620	9.8	- 3.6°	1000
4.55	19.5°	.564	8.8	- 0.9°	1990

waves originating at the equator. As demonstrated in Figure 6, rays starting at L ~ 4.5 cross the satellite track at L ~ 3.4. For the signal enhancement observed by S3-3 at L ~ 4.2, we assume that it is probably due to a reducted mode similar to the 'super whistler' mode discovered by Bernhardt (1979). However, we were not able to find the particular combination of starting L-shell, wave normal, duct parameters, etc., which would produce this ray path, so the assumed path is dotted in Figure 6.

Discussion

We have shown that (1) an enhancement of plasma sheet electrons existed above L ~ 4.35, (2) a detached region of the plasmasphere acted as a duct to allow the TVLF transmitter signals to propagate to the equatorial regions at L ~ 4.35 to L ~ 4.5, (3) for a reasonable density model the waves resonate with the whole range of low-energy electrons, and (4) the waves can propagate to the S3-3 satellite at low altitudes where they are observed from the duct leakage path and from the equator starting near L ~ 4.5.

It is instructive to examine the period about the observation on 2 August. Figure 7 plots Dst, Kp, and the location of the plasma sheet (~ 1 keV) electrons from 24 July to 4 August 1976. A moderately disturbed period started on 28 July and reached maximum Kp of 4+ on 30 July. Thereafter magnetic activity was unsettled until 5 August, with brief excursions of Kp to 4- on 2 and 4 August.

From 24 July to 4 August, S3-3 satellite real-time VLF wave and particle data were taken on daily passes (8-10 UT) through the plasmasphere at local evening (usually starting at L ~ 2 and terminating at L ~ 5-6). Supplementing these passes were four other passes at local evening which started at L ~ 4-5 and continued over the polar cap. These passes are arbitrarily terminated at L ~ 8 in Figure 7.

From July 24 to July 27, plasma sheet electrons were not observed although these passes were limited in coverage due to real-time telemetry tracking requirements. During this period, detached plasma regions were observed on two passes on 24-25 July. However, starting on 28 July during elevated Kp levels, plasma sheet electrons appear in some cases as a continuous region but

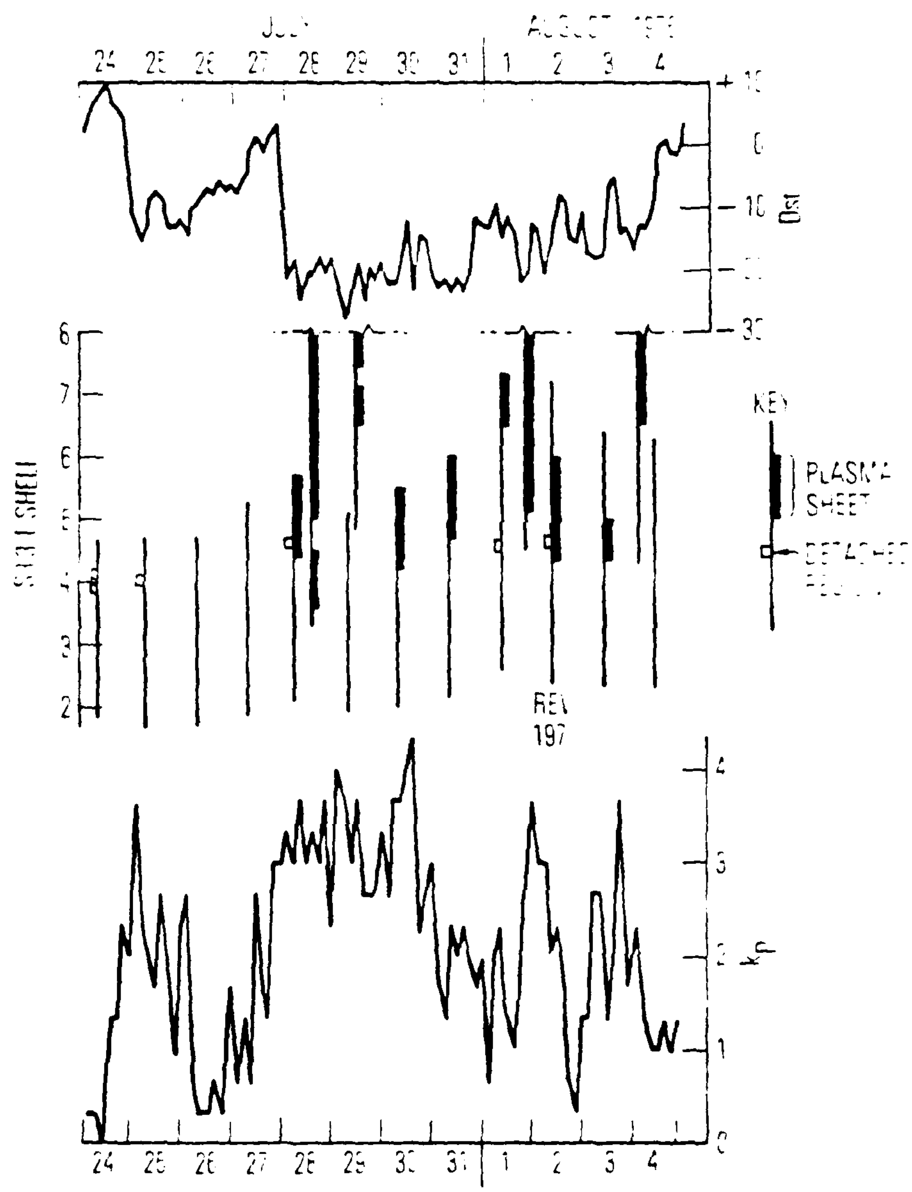

Figure 7. Dst and Kp indices for the period 24 July to 4 August 1976 and S3-3 orbit L-shell tracks showing plasma sheet locations and detached regions for the same period.

in other cases as an isolated region, separated from the main body of plasma sheet electrons at higher L-shells. A good example of the latter occurs on 28-29 July.

On the real-time passes on 30-31 July, we cannot tell whether the plasma sheet electrons observed are isolated or not because of the short pass length; but on 1 August the plasma sheet is observed at a higher L-shell than on the previous two days during a short period of magnetic quieting. However, on 2 August a plasma sheet region moved to L ~ 4.35 during a brief excursion of Kp to 4-.

Fennell et al. (1979) showed that the plasma sheet for a storm occurring in July 1977 moved inward to L ~ 4.5 in the late evening local time. Magnetic activity for that storm case study lasted only for two days, in contrast to the 8-day duration for the storm of this study. Fennell et al. (1979) also did not observe any isolated plasma sheet regions. Fennell (private communication) has not observed similar plasma sheet break ups in any other storms studied in the S3-3 satellite data.

The detached regions indicated in Figure 6 are consistent with the OGO observations of detached plasma regions described by Chappell (1974). The local time (~ 2000 LT) of the S3-3 observations of detached regions is near the peak occurrence time of 1600 LT reported by Chappell. Also, at local evening the OGO observations are centered about L ~ 4. The S3-3 observations are in the L-shell range of 4 to 5.

The occurrence of detached regions in the S3-3 data is somewhat irregular, as shown by Figure 7. We observed them during relatively quiet periods (e.g., 24-25 July) at the beginning of a storm (28 July) and during a period of irregular magnetic activity (1-2 August). The 1 August observation of a detached region at 62.7° invariant latitude is given by Figure 14 of Mozer (1979). The random occurrence of detached region observations in this period means that the overlap possibility of a detached region with plasma sheet is very infrequent. Besides, the 2 August event, the only other overlap occurred on 28 July. Unfortunately the transmitter was not operating for that pass.

The TVLF transmitter signal was observed in one other occasion after propagating in a detached region. This observation occurred on 2[illegible] July and [illegible]

discussed by Edgar (1980). For the 28 July storm, strong density gradients appeared at L ~ 4, but no evidence of transmitter paths guided by plasmapause gradients as shown by Inan et al. (1977) was observed.

Wave Observations

Another peculiar aspect about the S3-3 wave observatons was the appearance of strong emissions at frequencies other than the two transmitter frequencies (7.35 and 8.78 kHz). Koons et al. (1978) showed an amplitude-frequency scan about the lower transmitter frequency. A secondary peak appears at ~ 7.5 kHz. In Figure 1 these two frequencies appear at the beginning of the spectrogram at L ~ ^.9. The emission at 7.35 kHz soon dies away and the line at ~ 7.5 kHz continues in an irregular fashion till L ~ 3. At L ~ 2.9 a chorus band begins about the upper transmitter frequency at 8.78 kHz. which evolves into an emission band at 9.2 kHz. The same sequence of chorus emissions starts again at L ~ 3.0. At L ~ 3.15 an emission band structure appears between the upper and lower transmitter frequencies. This band structure ends at L ~ 3.3, and the chorus emissions about 9 kHz end about L ~ 3.4. The signal enhancement at L ~ 4.3 (not shown in Figure 1) occurs at f ~ 7.5 kHz. It is not clear from Figures 6 and 1 whether the emissions are temporally or spacially controlled as the spacecraft traverses the region. From the raytracing of Figure 6, the observational region between L ~ 2.9 and L ~ 3.3 is probably controlled by the spread of the raypaths, but the variation of the chorus bands may be both temporally and spacially controlled.

The S3-3 satellite also carried a broadband vlf magnetic wave receiver. However, the Magnetic Antenna data were contaminated by high EMI levels which were estimated to range between 100 and 250 m γ. But the vlf emissions associated with the higher frequency band of Figure 1 were strong enough to exceed the background noise threshold. The AGC of the magnetic receiver was calibrated for a single frequency input in m γ. However, the EMI consisted of four harmonically related frequencies whose amplitudes were within a few db of each other. Doing a R.M.S. summation of the relative amplitudes of the EMI signals and the chorus and normalizing to the magnetic field strength as given by the AGC, we estimate a value of 40 m γ (within a factor of 2) for the chorus magnetic field strength at 1130 UT (see Figure 1). The E field about this period was measured to be in the range of 100 to 200 uV/m. But due to the

transient nature of the chorus it was impossible to do simultaneous measurements of E and B for a meaningful refractive index calculation.

Conclusions

Further investigation of particle, density, and wave data from the S3-3 satellite for the 2 August 1976 wave amplification event reveals a unique situation where a detached region ducted vlf transmitter signals to a region where a wide range of plasma sheet electrons were in cyclotron resonance with the signals. The resultant emissions, ranging from emission bands to chorus, were observed by the low-altitude S3-3 satellite in a region which is consistent with duct leakage ray paths and emissions originating at the equator. Further, we have shown a new method of conveying VLF waves to a wave-particle interaction region which offers much promise for investigating the outer magnetosphere.

Bibliography

Bernhardt, P. A., Theory and analysis of the "super whistler", J. Geophys. Res., 84, 5131, 1979.

Chappell, C. R., Detached plasma regions in the magnetosphere, J. Geophys. Res., 79, 1861, 1974.

Edgar, B. C., Observation of amplified non-ducted whistler-mode waves from ground-based vlf transmitters, to be submitted to Radioscience, 1980.

Fennell, J. F., P. F. Mizera, and D. R. Corley, Observation of ion and electron distributions during the July 29 and July 30, 1977 storm period, Proceedings of Magnetospheric Boundary Layers Conference, Alpbach, 11-15 June 1979, ESA SP-148, 97, 1979.

Koons, H. C., M. H. Dazey, and B. C. Edgar, Satellite observation of discrete vlf line radiation within transmitter-induced amplification bands, J. Geophys. Res., 83, 3887, 1978.

Koons, H. C. and M. H. Dazey, Transportable VLF transmitter, in ELF-VLF Radio Wave Propagation, edited by J. A. Holtet, p. 417, D. Reidel, Dordrecht, Netherlands, 1974.

Inan, U. S., T. F. Bell, and R. R. Anderson, Cold plasma diagnostics using satellite measurements of vlf signals from ground transmitters, J. Geophys. Res., 82, 1167, 1977.

Mizera, P. F. and J. F. Fennell, Signatures of electric fields from high and low altitude particle distributions, Geophys. Res. Lett., 4, 311, 1977.

Mozer, F. S., C. Cattell, M. Termerin, R. B. Torbert, S. Von Glinski, M. Woldorff, and J. Wygant, The dc and ac electric field, plasma density, plasma temperature, and field-aligned current experiments on the S3-3 satellite, J. Geophys. Res., 84, 5875, 1979.

LABORATORY OPERATIONS

The Laboratory Operations of The Aerospace Corporation is conducting experimental and theoretical investigations necessary for the evaluation and application of scientific advances to new military space systems. Versatility and flexibility have been developed to a high degree by the laboratory personnel in dealing with the many problems encountered in the nation's rapidly developing space systems. Expertise in the latest scientific developments is vital to the accomplishment of tasks related to these problems. The laboratories that contribute to this research are:

Aerophysics Laboratory: Launch vehicle and reentry aerodynamics and heat transfer, propulsion chemistry and fluid mechanics, structural mechanics, flight dynamics; high-temperature thermomechanics, gas kinetics and radiation; research in environmental chemistry and contamination; cw and pulsed chemical laser development including chemical kinetics, spectroscopy, optical resonators and beam pointing, atmospheric propagation, laser effects and countermeasures.

Chemistry and Physics Laboratory: Atmospheric chemical reactions, atmospheric optics, light scattering, state-specific chemical reactions and radiation transport in rocket plumes, applied laser spectroscopy, laser chemistry, battery electrochemistry, space vacuum and radiation effects on materials, lubrication and surface phenomena, thermionic emission, photosensitive materials and detectors, atomic frequency standards, and bioenvironmental research and monitoring.

Electronics Research Laboratory: Microelectronics, GaAs low-noise and power devices, semiconductor lasers, electromagnetic and optical propagation phenomena, quantum electronics, laser communications, lidar, and electro-optics; communication sciences, applied electronics, semiconductor crystal and device physics, radiometric imaging; millimeter-wave and microwave technology.

Information Sciences Research Office: Program verification, program translation, performance-sensitive system design, distributed architectures for spaceborne computers, fault-tolerant computer systems, artificial intelligence, and microelectronics applications.

Materials Sciences Laboratory: Development of new materials: metal matrix composites, polymers, and new forms of carbon; component failure analysis and reliability; fracture mechanics and stress corrosion; evaluation of materials in space environment; materials performance in space transportation systems; analysis of systems vulnerability and survivability in enemy-induced environments.

Space Sciences Laboratory: Atmospheric and ionospheric physics, radiation from the atmosphere, density and composition of the upper atmosphere, aurorae and airglow; magnetospheric physics, cosmic rays, generation and propagation of plasma waves in the magnetosphere; solar physics, infrared astronomy; the effects of nuclear explosions, magnetic storms, and solar activity on the earth's atmosphere, ionosphere, and magnetosphere; the effects of optical, electromagnetic, and particulate radiations in space on space systems.

• • •